

State changing in Na(*nd*)-electron collisions

G. W. Foltz,* E. J. Beiting,† T. H. Jeys, K. A. Smith, F. B. Dunning, and R. F. Stebbings

*Department of Space Physics and Astronomy, Rice University, Houston, Texas 77001**and The Rice Quantum Institute, Houston, Texas 77001*

(Received 16 June 1981)

An experiment is described in which 25-eV electrons are allowed to collide with sodium atoms in selected *nd* Rydberg states with $36 \leq n \leq 50$. The excited collision products are analyzed by use of selective field ionization. Collisions are found to result in state changing, and cross sections for this process are estimated.

I. INTRODUCTION

The importance of interactions between charged particles and highly excited atoms in both astrophysical and laboratory plasmas has long been appreciated.^{1,2} Only recently, however, have experimental investigations of these interactions been undertaken. In several experiments involving collisions between positive ions and Rydberg atoms,³⁻⁶ the processes of impact ionization, charge transfer, and state changing have been observed and studied.

In the case of electron-Rydberg-atom collisions, only state changing processes have been studied to date. Schiavone *et al.*^{7,8} detected atoms in high-*l* Rydberg states following collisions between electrons and ground-state rare-gas atoms. They asserted that these atoms resulted not from direct excitation, which should favor the production of low-*l* states at the electron energies used,⁹ but rather from subsequent *l*-changing collisions between these low-*l* Rydberg atoms and electrons. Average cross sections for these *l*-changing processes were determined to be $\sim 10^{-10} - 10^{-9}$ cm². Atoms in high-*l* Rydberg states have also been observed by Kocher and Smith¹⁰ in experiments in which ground-state lithium atoms were excited to Rydberg states by electron impact at electron energies several times threshold. However, assuming that the observed high-*l* states did not result directly from excitation of ground-state atoms, these experiments were unable to determine whether the transition from low *l* to high *l* occurred through a single electron-Rydberg-atom collision in which a large change in angular momentum occurred, or through multiple collisions each involving only a small change in angular momentum. Recent theoretical studies by Flannery and McCann^{11,12} indicated that, in cer-

tain situations at least, large angular momentum changes might occur with reasonable probability.

Investigations of electron-induced *n*-changing collisions have been carried out by Delpech *et al.*¹³ and Devos *et al.*¹⁴ In these experiments metastable helium 2³S atoms in a helium afterglow were laser excited to single, well-defined *n* ³P Rydberg states ($8 \leq n \leq 17$) and allowed to collide with electrons. While the conditions in the afterglow prevented detailed examination of electron-induced *l*-changing collisions, it was, nevertheless, possible to observe *n*-changing collisions, and these were studied in detail. Rate constants as large as 10^{-4} cm³/sec were measured, and it was observed that $\Delta n > 1$ transitions were important.

The present paper reports a study of the interaction of sodium atoms in selected *nd* states with 25-eV electrons using a crossed-beams approach. The collision products were analyzed using selective field ionization (SFI).¹⁵⁻²⁰

II. APPARATUS AND EXPERIMENTAL METHOD

A schematic diagram of the apparatus is shown in Fig. 1. A beam of ground-state sodium atoms is produced by a conventional oven source and directed into a high-vacuum ($\sim 2 \times 10^{-8}$ Torr) chamber. The atoms then enter an interaction region between two planar, parallel grids where they are stepwise excited in zero (≤ 0.2 V cm⁻¹) electric field, via the intermediate $3p \ ^2P_{3/2}$ state, using the superposed outputs of two nitrogen-pumped dye lasers. The linewidths of the lasers permit excitation of single, selected *nd* Rydberg states for values of *n* up to about 50. The sodium beam has an estimated number density of $\sim 7 \times 10^6$ atoms/cm³ at the interaction region and is ultimately collected on a cooled surface.

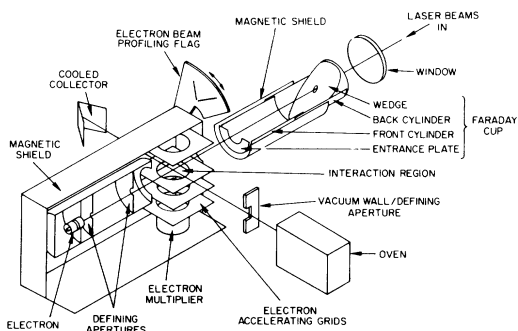


FIG. 1. Schematic diagram of apparatus.

The electron beam is collinear with, but oppositely directed to, the laser beams. The first three elements of a commercially available black-and-white television-tube electron gun provide the source of electrons. This gun produces a divergent electron beam which is collimated by defining apertures before entering the interaction region. The electron beam is ~ 1 cm in diameter at the interaction region (thereby totally immersing the Rydberg atoms in electrons) and is approximately uniform in number density. The position, size, and degree of uniformity of the beam were checked using a mechanical scanner.

The interaction region is maintained at ground potential during the laser pulse and the subsequent electron collisions. Thus the electron-beam energy is determined by the operating potential of the electron-gun cathode. Since the product states are analyzed by detection of the electrons produced by field ionization, the electron beam must be gated off during this measurement. This is accomplished by applying an appropriate voltage to the electron-gun control grid. In normal operation the electron beam is turned on ~ 2 μ sec before the laser pulse and turned off at the end of the interaction interval, t_I , whereupon the Rydberg atom population is analyzed.

Following its intersection with the sodium beam, the electron beam enters a Faraday cup which is used to measure the beam current. This cup consists of an entrance plate, two overlapping cylinders, and a wedge-shaped back surface. The cup lies on the common axis of the electron and laser beams and has an orifice in its back surface through which the laser beam passes. The back cylinder is operated at $+150$ V while the other three elements of the cup are held at ground potential. Thus, the electron beam, once inside the cup, is deflected from the beam axis onto the back cylinder. The electron-beam current during the

beam pulse is measured by dividing the time-averaged sum of the currents to the cup elements by the duty cycle of the beam. The beam current during the pulse is $\lesssim 1$ μ A.

Care was taken in the design and operation of the electron beamline to minimize the number of low-energy scattered or secondary electrons in the interaction region. A subsidiary experiment in which such electrons were allowed to drift to the electron multiplier indicated that they were few in number.

The electron gun, interaction region, and Faraday cup are all located in μ -metal enclosures to exclude the Earth's magnetic field. Care is also taken to minimize stray electric fields in the interaction region since even small fields influence both excitation and collision processes.^{15,16} To this end the grid immediately below the interaction region is constructed of fine wire mesh (100 wires/in.) in order to reduce field penetration resulting from the voltages applied to the electron multiplier and electron acceleration grids below the interaction region. The entrance plate and first cylinder of the Faraday cup are also held at ground potential to reduce penetration effects. In addition, no effects of importance to the present work were observed in a subsidiary experiment in which Rydberg atoms were intentionally excited in the presence of small ($\lesssim 5$ V/cm) applied electric fields.

The laser-excited atoms and the excited collision products are detected and identified by use¹⁵⁻²⁰ of SFI for which purpose a pulsed electric field that rises from 0 to $\lesssim 1000$ V/cm in ~ 1 μ sec is applied across the interaction region. This field is generated by application of equal, but opposite polarity, voltage ramps to the grids on either side of the interaction region. The electrons liberated at ionization are thereby accelerated to an electron multiplier whose output is fed to a time-to-amplitude converter (TAC). The TAC is started at the beginning of the ionizing voltage ramp and is stopped by the first electron pulse subsequently registered by the detector. The TAC output is fed to a standard multichannel pulse analyzer (MCA). For sufficiently low count rates ($\lesssim 0.1$ per laser pulse) the MCA stores a signal proportional to the probability of a field ionization event per unit time during the ramp. The probability of field ionization per unit field increment may be derived from the measurement of the time dependence of the ionizing field.

Since atoms in different Rydberg states ionize at different field strengths, it is in principle possible

to infer from SFI data the state distribution of the Rydberg-atom population. However, in order to identify a given SFI feature with a particular zero-field Rydberg state, the nature of the path of ionization must be completely known. Previous studies^{15–20} have shown that, in an increasing field, sodium Rydberg atoms typically follow either predominantly adiabatic or diabatic paths to ionization. For sodium *nd* atoms, and the ionizing field slew rates employed in this study, atoms with $|m_l| \leq 1$ ionize predominantly adiabatically while those with $|m_l| > 1$ ionize predominantly diabatically.

In order to identify effects due to collisions with electrons, it is necessary to determine and correct for effects due to collisions with background gas, and effects due to interactions with background thermal radiation. To accomplish this, data are recorded under three different conditions. In the first measurement the laser-excited Rydberg atoms are allowed to interact with electrons for a time $t_I = 6 \mu\text{sec}$ following which the Rydberg-atom population is analyzed by SFI. The second measurement is conducted similarly except that the sodium beam is turned off in order to identify spurious signals associated with the electron beam. This background is then subtracted channel-by-channel from the first measurement to give the electron-beam-on data. In the third measurement the electron beam is turned off so that background effects due to processes involving Rydberg atoms can be identified. In order to ensure that these three measurements pertain to the same initial Na(*nd*) population and electron-beam current, data for a given *nd* state are obtained by repeatedly alternating these measurements, each for an equal number of laser pulses.

The present experiments are undertaken with very small electron-beam currents and, in consequence, only a small number of state-changed collision products are formed. Thus, the differences between the SFI spectra obtained with and without the electron beam are very small and the product atoms must be detected in the presence of a much larger number of remaining parent Rydberg atoms. Typically, fewer than 10% of the parent atoms undergo a state-changing collision in the interval t_I .

III. RESULTS AND DISCUSSIONS

Representative SFI spectra [for Na(36*d*) and Na(50*d*)] are shown in Figs. 2(a) and 3(a). The data obtained with the electron beam gated off

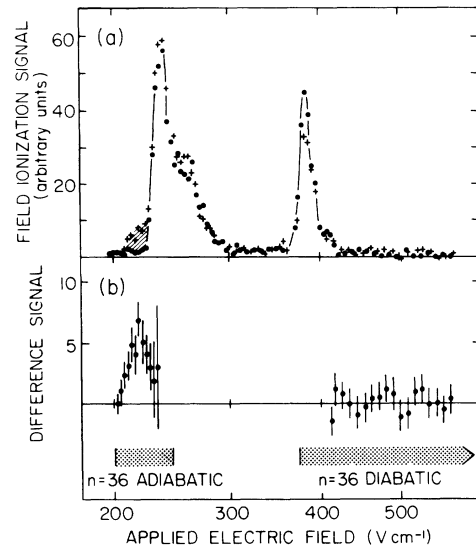


FIG. 2. Typical SFI data for laser-excited Na(36*d*) atoms: (a) ● data with electron beam gated off; + data following collisions with 25-eV electrons, corrected for electron-induced background signals. (b) Net signal due to electron impact. The horizontal bars indicate the range of field strengths over which $n=36$ atoms are expected to ionize adiabatically and diabatically.

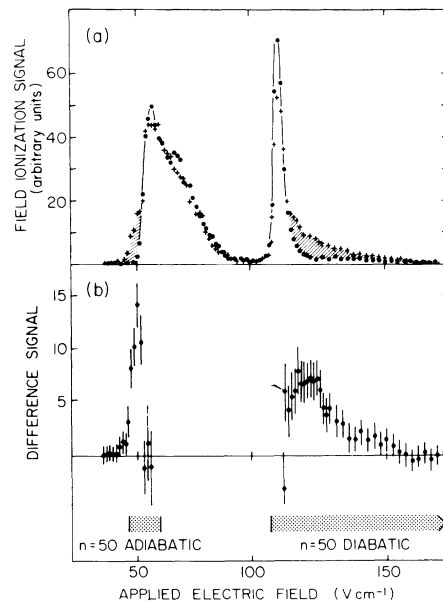


FIG. 3. Typical SFI data for laser excited Na(50*d*) atoms: (a) ● data with electron beam gated off; + data following collisions with 25-eV electrons, corrected for electron-induced background signals. (b) Net signal due to electron impact. The horizontal bars indicate the range of field strengths over which $n=50$ atoms are expected to ionize adiabatically and diabatically.

result primarily from ionization of the laser-excited Rydberg atoms, although there is a small contribution from atoms in states populated by background-induced state-changing processes. Two major SFI features are observed^{15–17} in each spectrum. The low-field ionization feature results from the predominantly adiabatic ionization of states with $|m_l| = 0, 1$, while the high-field feature is produced by predominantly diabatic ionization of states with $|m_l| = 2$.

The SFI profiles obtained following electron impact are corrected as described above for spurious effects due to the electron beam and thus result from field ionization of laser-excited Rydberg atoms and of atoms in states populated through both electron and background interactions. Comparison of the two spectra in part (a) of each figure shows that collisions with electrons result in enhanced field ionization signals—shown shaded—at certain values of applied field. The net signal resulting from electron collisions in these regions is shown on an enlarged scale in part (b) of each figure. Since the lifetimes of the parent and product atoms are typically much longer than the interaction time, signal enhancement at certain values of the applied field is necessarily accompanied by signal reduction at other field strengths. Inspection of Figs. 2(a) and 3(a) reveals regions where the electron-beam-off signal exceeds the electron-beam-on signal.

The electron-impact-induced field ionization signals which appear on the low-field side of the parent nd adiabatic features result from adiabatic ionization of atoms either in the neighboring $(n+1)p$ state or in low $|m_l|$, nl ($l > 2$) states. A more precise identification is not possible because

SFI studies showed that these would both yield ionization signals over this range of field strengths.²¹ At the lower values of n studied, the data do not suggest significant population of high- l nl states since in these circumstances a diabatic signal would also be apparent.¹⁶ However, at higher n a diabatic electron-impact-induced field ionization signal is observed. Its width indicates that collisions lead to a broad range of state-changed atoms with high l .¹⁶ Attempts were made to determine whether these high- l products resulted from single or multiple collisions by making measurements at several electron-beam currents. These studies suggest that the high- l states result from single collisions, although the small size of the signals make a definitive determination impossible. However, since only a few percent of the laser-excited atoms undergo state changing, the evidence suggests that single-collision conditions pertain and that collisions populate high- l states directly. No SFI features ascribable to n -changing collisions, other than the feature mentioned earlier that could possibly result from $nd \rightarrow (n+1)p$ collisions, are apparent.

Cross sections σ for the state-changing process are estimated by determining the number of state-changed atoms, $N_{sc}(t_I)$, comprising the shaded region in Figs. 2(a) and 3(a), resulting from electron collisions in the time t_I . Neglecting the (very small) radiative decay of parent and product atoms during the interval t_I , $N_{sc}(t_I)$ and $N_p(0)$, the initial parent nd population, are related by

$$\frac{N_{sc}(t_I)}{N_p(0)} = n_e \sigma v t_I,$$

where n_e is the number density of electrons and v

TABLE I. Compilation of measured and calculated l -changing cross sections in cm^2 for collisions between $\text{Na}(nd)$ atoms and 25-eV electrons.

n	Present results	Percival and Richards ^a		Herrick ^b
		$nd \rightarrow (n+1)p$	$nd \rightarrow nf$	$nd \rightarrow nf$
35		8.7×10^{-10}	2.1×10^{-9}	2.0×10^{-9}
36	6.6×10^{-10}			
38	5.7×10^{-10}			
40	1.5×10^{-9}	1.5×10^{-9}	3.6×10^{-9}	3.5×10^{-9}
41	2.3×10^{-9}			
45	3.0×10^{-9}	2.5×10^{-9}	5.8×10^{-9}	5.7×10^{-9}
50 ^c	3.4×10^{-9}	3.9×10^{-9}	9.0×10^{-9}	8.9×10^{-9}

^aReference 22.

^bReference 23.

^cA small number of $(n+1)s$ states may also be produced by the laser.

is the relative Rydberg atom-electron collision velocity. $N_p(0)$ is determined by integrating over the SFI spectrum obtained in the absence of electrons. The value of n_e is obtained from the measurement of the electron-beam pulse current, the cross-sectional area, and the known electron energy. Cross sections derived in this manner for an electron energy of 25 eV are given in Table I. These cross sections provide a lower bound to the total state-changing cross sections since a fraction of the state-changed atoms may ionize at the same time field strengths as parent *nd* atoms. Such atoms would go undetected and are thus not included in $N_{sc}(t_I)$. However, reasonable estimates based on the known shapes of SFI profiles for *p* states and for the state-changed products resulting from neutral collisions suggest that, at most, this should lead to an underestimate of $N_{sc}(t_I)$ of no more than a factor of 3.

Theoretical values^{22,23} for various state-specific collision processes are also included in Table I. Radial matrix elements extrapolated from the results of Gounand²⁴ were used in conjunction with the theory of Percival and Richards²² to determine the $nd \rightarrow nf$ and $nd \rightarrow (n+1)p$ cross sections. $nd \rightarrow nf$ cross sections were also derived using the theory of Herrick²³ and the quantum defects for sodium *d* and *f* states. The present data are in reasonable accord with the theoretical values. However, the theoretical treatments consider only dipole-allowed, i.e., $\Delta l = \pm 1$, transitions and the present SFI data suggest that, certainly at higher *n*, larger changes in Δl are possible.

This work was supported by the National Science Foundation under Grant No. PHY78-09860 and by the Robert A. Welch Foundation.

*Present address: Health & Safety Research Division, Oak Ridge National Laboratory, Oak Ridge, Tennessee 37830.

†Present address: Physics Department, Mississippi State University, Mississippi 39762.

- ¹D. R. Bates, A. E. Kingston, and R. W. P. McWhirter, Proc. R. Soc. London A 267, 297 (1962).
- ²D. R. Bates, A. E. Kingston, and R. W. P. McWhirter, Proc. R. Soc. London A 270, 155 (1962).
- ³P. M. Koch and J. E. Bayfield, Phys. Rev. Lett. 34, 448 (1975).
- ⁴M. Burniaux, F. Brouillard, A. Jognaux, T. R. Govers, and S. Szucs, J. Phys. B 10, 2421 (1977).
- ⁵K. B. MacAdam, D. A. Crosby, and R. Rolfes, Phys. Rev. Lett. 44, 980 (1980).
- ⁶H. J. Kim and F. W. Meyer, Phys. Rev. Lett. 44, 1047 (1980).
- ⁷J. A. Schiavone, D. E. Donohue, D. R. Herrick, and R. S. Freund, Phys. Rev. A 16, 48 (1977).
- ⁸J. A. Schiavone, S. M. Tarr, and R. S. Freund, Phys. Rev. A 20, 71 (1979).
- ⁹U. Fano, J. Phys. B 7, L401 (1974).
- ¹⁰C. Kocher and A. Smith, Phys. Lett. 61A, 305 (1977).
- ¹¹M. R. Flannery and K. J. McCann, J. Phys. B 12, 427 (1979).
- ¹²M. R. Flannery and K. J. McCann, Astrophys. J. 236, 300 (1980).
- ¹³J.-F. Delpech, J. Boulmer, and F. Devos, Phys. Rev. Lett. 39, 1400 (1977).
- ¹⁴F. Devos, J. Boulmer, and J.-F. Delpech, J. Phys. (Paris) 40, 215 (1979).
- ¹⁵T. H. Jeys, G. W. Foltz, K. A. Smith, E. J. Beiting, F. G. Kellert, F. B. Dunning, and R. F. Stebbings, Phys. Rev. Lett. 44, 390 (1980).
- ¹⁶F. G. Kellert, T. H. Jeys, G. B. McMillian, K. A. Smith, F. B. Dunning, and R. F. Stebbings, Phys. Rev. A 23, 1127 (1981).
- ¹⁷T. H. Jeys, G. B. McMillian, K. A. Smith, F. B. Dunning, and R. F. Stebbings (unpublished).
- ¹⁸T. F. Gallagher, M. L. Humphrey, R. M. Hill, and S. A. Edelstein, Phys. Rev. Lett. 37, 1465 (1976).
- ¹⁹T. F. Gallagher, M. L. Humphrey, W. E. Cooke, R. M. Hill, and S. A. Edelstein, Phys. Rev. A 16, 1098 (1977).
- ²⁰F. G. Kellert, K. A. Smith, R. D. Rundel, F. B. Dunning, and R. F. Stebbings, J. Chem. Phys. 72, 3179 (1980).
- ²¹The high-*l* states were populated by Na(*nd*)-neutral collisions, the *p* states by blackbody-induced photoexcitation from laser-excited *ns* states.
- ²²I. C. Percival and D. Richards, J. Phys. B 10, 1497 (1977).
- ²³D. R. Herrick, Mol. Phys. 35, 1211 (1978).
- ²⁴F. Gounand, J. Phys. (Paris) 40, 457 (1979).